Inorg. Chem. **2008**, *47*, 2576−2580

Metal Effects on Electronic Structures of Directly Linked Tribenzotetraazachlorin-Fullerene Conjugates

Takamitsu Fukuda, **Satoshi Masuda**, **Naoaki Hashimoto**, **and Nagao Kobayashi***

Department of Chemistry, Graduate School of Science, Tohoku University, Sendai 980-8578, Japan

Received September 18, 2007

Mixed condensation of 1,2-dicyanofullerene (**1**) and 4,5-dibutyloxyphthalonitrile (**2a**) in the presence of vanadium(III) chloride (VCl_3) in quinoline forms the hexabutyloxy-substituted tribenzotetraazachlorin (TBTAC) - fullerene (C_{60}) vanadyl complex (**3**). UV–vis absorption and magnetic circular dichroism (MCD) spectroscopy demonstrated that **3** shows two intense Q-band components, whereas the previously reported nickel complex possessing the identical peripheral substituents (**4**) shows one intense and two medium-intense bands in the 600–800 nm region, indicating that the electronic mixing states of **3** are different from those of the nickel complex (**4**). The metal effects on electronic structures of the conjugates were interpreted using density functional theory (DFT) calculations.

Introduction

Phthalocyanines (Pcs) are one of the most robust and versatile heteroaromatic compounds known to date. Recently, there has been an increasing focus on Pcs in applications such as photovoltaic cells, molecular electronics, photosensitizers, and electrochromic materials.[1] Tetraazachlorin (TAC) derivatives are partially ring-hydrogenated Pc analogues, and potential applications of TACs extend into numerous industrial areas owing to their rich photo and electro active character. In addition, their structures enable functional moieties to be linked at the periphery of the TAC skeleton, due to the presence of sp^3 carbons at the reduced sites. The first attempts to synthesize the TAC skeleton were pioneered by Linstead et al. in the late 1950s, in which catalytic hydrogenation of alkyl-substituted magnesium tetraazaporphyrins (TAPs) was carried out.[2] However, their compounds are unstable and spontaneously oxidized to give rise to the TAP skeleton or even decomposed species. Recently, one of our group has developed the effective synthetic protocols of stable TBTAC derivatives by using tetramethylsuccinonitrile as a source of the hydrogenated sites.[3] Of particular interest to us is the introduction of the fullerene (C_{60}) moiety as a functional unit because TBTAC-C_{60} conjugates appear to be promising candidates for realizing strongly interacting π-electron systems, if molecular orbitals (MOs) of the TBTAC and C_{60} have the correct symmetry and two constituting units are disposed in close proximity.[4–6] We revealed in our recent study that highly interacting NiT-BTAC-C_{60} conjugates can be synthesized by condensing 1,2-dicyanofullerene (**1**) and phthalonitrile derivatives in the presence of nickel chloride.[7] The electronic structures of the conjugates depended significantly on the electron donating/withdrawing nature of the peripheral substituents of the

* To whom correspondence should be addressed. nagaok@mail.tains.tohoku.ac.jp. Tel/fax: 81-22-795-7719.

(1) (a) Leznoff, C. C., Lever, A. B. P., Eds. *Phthalocyanines: Properties and Applications*; Wiley-VCH: New York, 1989–1996; Vols. 1–4. (b) Kadish, K. M., Smith, K. M., Guilard, R., Eds. *The Porphyrin Handbook*; Academic Press: San Diego, 2003; Vols. 15–20.

(2) Ficken, G. E.; Linstead, R. P.; Stephen, E.; Whalley, M. *J. Chem. Soc.* **1958**, 3879.

(3) (a) Makarova, E. A.; Fukuda, T.; Luk'yanets, E. A.; Kobayashi, N. *Chem.—Eur. J.* **2005**, *11*, 1235. (b) Fukuda, T.; Makarova, E. A.; Luk'yanets, E. A.; Kobayashi, N. *Chem.—Eur. J.* **2004**, *10*, 117. (c) Makarova, E. A.; Korolyova, G. V.; Tok, O. L.; Luk'yanets, E. A. *J. Porphyrins Phthalocyanines* **2000**, *4*, 525. (d) Miwa, H.; Makarova, E. A.; Ishii, K.; Luk'yanets, E. A.; Kobayashi, N. *Chem.—Eur. J.* **2002**, *8*, 1082.

(4) Mizuseki, H.; Igarashi, N.; Bilosludov, R. V.; Farajian, A. A.; Kawazoe, Y. *Synth. Met.* **2003**, *138*, 281.

(5) (a) Guldi, D. M.; Gouloumis, A.; Vázquez, P.; Torres, T.; Vasilios, G.; Prato, M. *J. Am. Chem. Soc.* **2005**, *127*, 5811. (b) Torres, T.; Gouloumis, A.; Sanchez-Garcia, D.; Jayawickramarajah, J.; Seitz, W.; Guldi, D. M.; Sessler, J. L. *Chem. Commun.* **2007**, 292. (c) Guldi, D. M.; Zilbermann, I.; Gouloumis, A.; Vázquez, P.; Torres, T. *J. Phys. Chem. B* **2004**, *108*, 18485. (d) Gouloumis, A.; Liu, S. -G.; SastreÁ.; Vázquez, P.; Echegoyen, L.; Torres, T *Chem.—Eur. J.* **2000**, *6*, 3600. (e) Linssen, T. G.; Dürr, K.; Hanack, M.; Hirsch, A. *J. Chem. Soc., Chem. Commun.* **1995**, 103.

(6) Guldi, D. M.; Rahman, G. M. A.; Marczak, R.; Matsuo, Y.; Yamanaka, M.; Nakamura, E. *J. Am. Chem. Soc.* **2006**, *128*, 9420.

(7) Fukuda, T.; Masuda, S.; Kobayashi, N. *J. Am. Chem. Soc.* **2007**, *129*, 5472.

10.1021/ic701840r CCC: $40.75
Published on Web 03/08/2008

Scheme 1. Synthetic Procedures for **3**−**5**

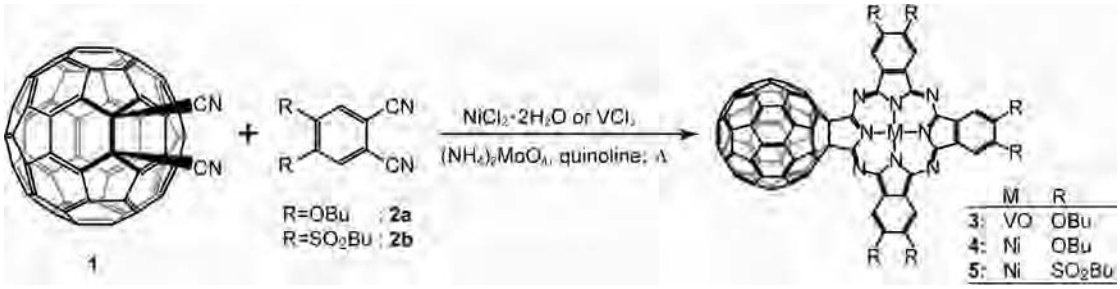

NiTBTAC moiety. The butyloxy (OBu)-substituted conjugate, **4**, had some MOs delocalized over the entire molecule, while the electron withdrawing butylsulfonyl (SO_2Bu)-substituted analogue, **5**, did not have delocalized frontier MOs. As a consequence, we were able to control the electronic communications on and off by changing the peripheral substituents, even though the aromatic skeletons of these were identical.[7]

In this paper, we describe the synthesis of a vanadyl complex of the TBTAC-C_{60} conjugate, **3** (Scheme 1), derived from the corresponding dinitriles and vanadium chloride (VCl_3), and the investigation of metal effects on the electronic structures of the conjugates. Interestingly, as will be shown below, the central metal has pronounced effects on the electronic structures of the conjugates.

Experimental Section

Instrumentation. High-resolution electron spray ionization Fourier transform ion cyclotron resonance (ESI-FTICR) mass spectra were measured with a Bruker APEX III spectrometer. Electronic absorption spectra were measured with a Jasco V-570 spectrophotometer. Magnetic circular dichroism (MCD) spectra were run on a Jasco J-725 spectrodichrometer with a Jasco electromagnet that produced a magnetic field of up to 1.09 T. The magnitude of MCD features are expressed in terms of molar ellipticity per tesla, $[\theta]_M$ (deg mol^{-1} dm^3 cm^{-1} T^{-1}). FTIR spectra were recorded on a Jasco FT/IR-4200 spectrometer. Cyclic voltammograms and differential pulse voltammograms were recorded using a Hokuto Denko HZ-5000 electrochemical analyzer. A glassy carbon working electrode and a platinum wire counter electrode were used. The reference electrode was Ag/AgCl, corrected for junction potentials by being referenced internally to the ferrocenium/ferrocene (Fc^+/Fc) couple.

Computational Method. The Gaussian 03 program[8] was used to perform DFT calculations. Deconvolution of the pairs of associated absorption and MCD spectral data was carried out by using the SIMPFIT program.[9]

Synthesis. 1,2-dicyanofullerene (**1**) and 4,5-dibutyloxyphthalonitrile (**2a**) were prepared by the method of Wudl et al.[10] and Nolte et al.,[11] respectively.

Preparation of 3. A mixture of **1** (100 mg, 0.13 mmol), **2a** (70 mg, 0.26 mmol), VCl_3 (22 mg, 0.14 mmol), and a catalytic amount of ammonium molybdate (7.6 mg, 0.039 mmol) dispersed in freshly distilled quinoline (1 mL) was heated at 250 °C with stirring in an argon atmosphere, and urea (40 mg, 0.67 mmol) was added. After 2 h, the mixture was cooled to room temperature and dispersed in methanol. The resultant precipitate was filtered off and dried under reduced pressure. The crude solid was chromatographed successively using silica ($CHCl_3$, Rf = 0.32), alumina ($CHCl_3$, Rf = 0.93), and Biobeads S-x1 (Biorad, $CHCl_3$). Recrystallization from $CHCl_3$/MeOH gave **3** as a green solid (21 mg) in 13% yield. MASS (High-resolution FT-ICR): *m*/*z* 1655.4032 (M^+); calcd, 1655.4019. IR (KBr): 745, 858, 898, 1007 (V═O), 1034, 1070, 1094, 1107, 1202, 1277, 1328, 1383, 1416, 1464, 1483, 1510, 1552, 1604 cm^{-1}. Anal. Found: C, 79.64; H, 3.51; N, 6.35. Calcd for $C_{110}H_{60}N_8O_7V$: C, 79.75; H, 3.65; N, 6.76.

Results and Discussion

Synthesis and Characterization. In our previous papers,[3a,b] we reported that TBTAC and its related aromatic compounds such as dibenzotetraazabacteriochlorin (DBTABC) or dibenzotetraazaisobacteriochlorin (DBTAiBC) can be obtained by the mixed condensation of phthalonitrile and tetramethylsuccinonitrile. Although either lithium-mediated reaction (lithium method) or metal template reaction can be employed for the macrocyclization, the lithium method is superior in order to obtain a series of metal complexes, because a variety of metal ions can be incorporated to metal free macrocycles. However, undesired side-reactions at the C_{60} moiety caused in the applied reaction conditions exclude the use of the lithium method for the synthesis of TBTAC-C_{60} conjugates. Metal template reactions yield the corresponding metallo TBTAC-C_{60} conjugates with reasonable yields, although only nickel and vanadyl complexes can be currently available for the synthesis of TBTAC.[3b] In fact, several attempts to synthesize copper and zinc complexes were unsuccessful. Therefore, we decided to synthesize

(8) Frisch M. J.; Trucks G. W.; Schlegel H. B.; Scuseria G. E.; Robb M. A.; Cheeseman J. R.; Montgomery J. A., Jr.; Kudin K. N.; Burant J. C.; Millam J. M.; Iyengar S. S.; Tomasi J.; Barone V.; Mennucci B.; Cossi M.; Scalmani G.; Rega N.; Petersson G. A.; Nakatsuji H.; Hada M.; Ehara M.; Toyota K.; Fukuda R.; Hasegawa J.; Ishida M.; Nakajima T.; Honda Y.; Kitao O.; Nakai H.; Klene M.; Li X.; Knox J. E.; Hratchian H. P.; Cross J. B.; Adamo C.; Jaramillo J.; Gomperts R.; Stratmann R. E.; Yazyev O.; Austin A. J.; Cammi R.; Pomelli C.; Ochterski J. W.; Ayala P. Y.; Morokuma K.; Voth G. A.; Salvador P.; Dannenberg J. J.; Zakrzewski V. G.; Dapprich S.; Daniels A. D.; Strain M. C.; Farkas O.; Malick D. K.; Rabuck A. D.; Raghavachari K.; Foresman J. B.; Ortiz J. V.; Cui Q.; Baboul A. G.; Clifford S.; Cioslowski J.; Stefanov B. B.; Liu G.; Liashenko A.; Piskorz P.; Komaromi I.; Martin R. L.; Martin D. J.; Fox D. J.; Keith T.; Al-Laham M. A.; Peng C. Y.; Nanayakkara A.; Challacombe M.; Gill P. M. W.; Johnson B.; Chen W.; Wong M. W.; Gonzalez C.; Pople J. A. *Gaussian 03, Revision B.05*, Gaussian, Inc.: Pittsburgh, PA, 2003.

(9) (a) Kobayashi, N.; Fukuda, T.; Lelièvre, D. *Inorg. Chem.* **2000**, *39*, 3632. (b) Browett, W. R.; Stillman, M. J. *J. Comput. Chem.* **1987**, *11*, 73.

(10) Keshavarz, K. M.; Knight, B.; Srdanov, G.; Wudl, F. *J. Am. Chem. Soc.* **1995**, *117*, 11371.

(11) van der Pol, J. F.; Neeleman, E.; Zwikker, J. W.; Nolte, R. J. M.; Drenth, W. *Recl. Trav. Chim. Soc., Pays-Bas* **1988**, *107*, 615.

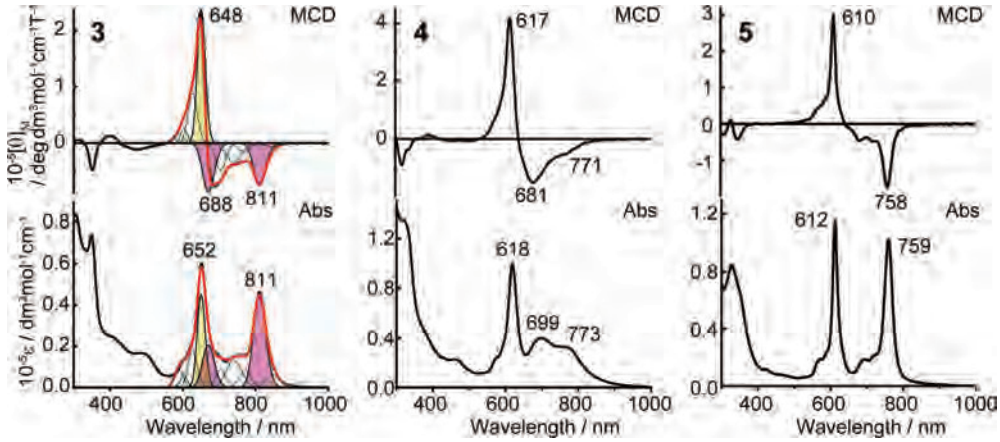

Figure 1. MCD (top) and absorption (bottom) spectra of **3** (left), **4** (middle), and **5** (right) in $CHCl_3$. Deconvoluted Gaussian curves and the simulated spectra for **3** are shown by the dotted and red solid lines, respectively, with assigned Q-band components represented by the colored Gaussians.

vanadyl complex of the TBTAC-C_{60} conjugate as the purpose of this study. Mixed condensation of **1**, **2a**, and VCl_3 was conducted at 250 °C in the presence of ammonium molybdate (Scheme 1). Compound **3** was identified by elemental analysis, IR and HRMS. Since vanadyl complexes are paramagnetic, NMR can not be employed for the structural characterizations. Typical vanadyl Pc shows the V=O stretching mode at 1005 cm^{-1} in the IR spectrum,[12] and a similar band was observed for vanadyl porphyrins at around 1000 cm^{-1}.[13] Therefore, the medium-intense IR absorption at 1007 cm^{-1} for **3** is indicative of the VO moiety in the conjugate (see the Supporting Information). Using ESI ionization with sodium iodide as an additive, the parent ion and its sodium adduct were readily detected at 1655.4032 (*m*/*z*) and 1678.3928 (*m*/*z*), respectively, unambiguously confirming the formation of **3**. No DBTABC and DBTAiBC complexes were isolated.

Spectroscopy. The absorption and MCD spectra of **3**-**5** in $CHCl_3$ are shown in Figure 1. While the nickel derivative, **4**, shows one medium intensity band at 618 nm and two weaker bands in the 700–900 nm region, the VO complex, **3**, shows two sharp absorption bands at 652 and 811 nm. The absorption band envelopes of **3** are, therefore, reminiscent of those of **5**, in which two intense absorption bands at 612 and 759 nm are attributed mainly to the HOMO to LUMO+1, and HOMO to LUMO transitions.[7] However, the MCD spectra indicate that the electronic structure of **3** is not identical to those of **5**. Two distinct oppositely signed Faraday *B*-terms are obtained for the two split absorption bands of **5**, while the MCD signal corresponding to the absorption band at 652 nm of **3** looks like a dispersion type. The Q-band region was deconvoluted simultaneously for both the absorption and MCD spectra using the same band-center and bandwidth parameters (the obtained band components are shown by Gaussian curves in Figure 1). The results indicate that the Q-band region consists of three principal absorption bands at 650, 670, and 810 nm (shown as colored Gaussians in Figure 1). Corresponding to the bands at 670 and 810 nm, negative MCD envelopes were detected, whereas a positive MCD signal was observed for the band at 650 nm. Therefore, it is conceivable that the MOs of the former two bands are parallel to each other, while these are normal to the 650 nm band.[14]

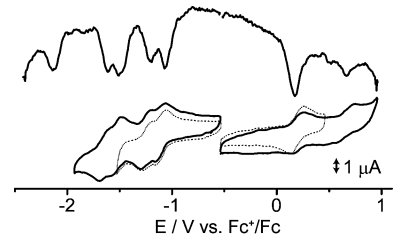

Figure 2. Cyclic voltammograms (bottom) and differential pulse voltammograms (top) of **3** in *o*-DCB containing 0.1 M TBAP. The dotted lines were recorded in a smaller potential window in order to confirm the reversibility of the redox processes.

Table 1. Redox Potentials/V vs Fc^+/Fc in *o*-DCB Containing 0.1 M TBAP

compd	fifth red	fourth red	third red	second red	first red	first ox	second ox
3[a]	−2.15	−1.62	−1.52	−1.20	−1.08	0.17	0.66
4[b]			−1.69	−1.45	−1.11	0.13	0.64
5[b]	−1.93	−1.51	−1.14	−1.08	−0.62	0.78	
C_{60}[b]		−2.36	−1.90	−1.46	−1.07		
$C_{60}(Me)_2$[c]			−2.00	−1.45	−1.03		

[a] Data from DPV. [b] See ref 7. [c] Data recorded in benzonitrile. See: Caron, C.; Subramanian, R.; D'Souza, F.; Kim, J.; Kutner, W.; Thomas Jones, M.; Kadish, K. M. *J. Am. Chem. Soc.* **1993**, *115*, 8505.

Electrochemistry. Cyclic voltammetry (CV) and differential pulse voltammetry (DPV) in *o*-dichlorobenzene (*o*-DCB) containing 0.1 M tetrabutylammonium perchlorate (TBAP) revealed that the TBTAC-centered first and second oxidation potentials of **3** are shifted positively with respect to that of **4** by about 40 and 20 mV, respectively, indicating that the VO complex has a stronger electron-deficient character compared to the nickel complex (Figure 2 and Table 1). The first oxidation couples of **3** seem to be irreversible since the corresponding cathodic current is lost (Figure 2, solid line). However, the dotted line shows this process is reversible ($i_{pa}/i_{pc} = 1.0$) if the sweep is reversed

(12) Assour, J. M.; Goldmacher, J.; Harrison, S. E. *J. Chem. Phys.* **1965**, *43*, 159.

(13) Erdman, J. G.; Ramsey, V. G.; Kalenda, N. W.; Hanson, W. E. *J. Am. Chem. Soc.* **1956**, *78*, 5844.

(14) MCD theory suggests that oppositely signed Faraday *B*-terms are expected if a transition couples with one that is orthogonal to it.

at 1.0 V (vs Ag/AgCl), suggesting that the second oxidation state of **3** is unstable. Similar instability of the second oxidation state was also observed for **4**.[7] Compound **3** shows five reduction couples at −1.08, −1.20, −1.52, −1.62, and −2.15 V vs Fc^+/Fc. Because VOPc shows no metal-centered redox couples,[15] these are all attributable to the reduction of TBTAC or C_{60} moieties. The reversibility of the reduction couples is ambiguous because of the overlap of more than one redox couples on the cyclic voltammograms. Nevertheless, the first and second reduction couples look reversible. Although VO can be formally regarded as an electron withdrawing unit in comparison with nickel, it is not as strong as that induced by the six SO_2Bu groups.[7,16] The MOs of the conjugates can be expressed as the linear combinations of the MOs of the constituent TBTAC and C_{60} moieties. If the associated MOs of the constituent units are energetically close, larger MO mixings are expected for the corresponding MOs of the conjugate. The results of electrochemistry indicate that the TBTAC moiety of the vanadyl complex, **3**, has lower MO energies compared to the nickel complex, **4**. Compound **5** is known to show practically no MO mixing. Therefore, it is conceivable that the degree of the MO mixing between the constituting units of **3** lies between that of **4** and **5**. The details of the MO mixings will be discussed in the subsequent section.

DFT Calculations. To understand how the electronic structure is perturbed by the central metal, DFT calculations were performed. The molecular geometries were first optimized at the B3LYP/3–21G combination of the hybrid functional and basis set, followed by single point calculations within the unrestricted B3LYP/6–31G(d) level. As mentioned in our previous paper,[7] the calculations on unsubstituted conjugates reproduce well the electronic structures of OBu-substituted conjugates. Although the calculated α and β orbital energies are not identical due to the paramagnetic nature of **3**, the energy differences between these are very small. For example, the orbital energies of HOMO(α) and LUMO(α) are calculated to be −0.19423 hartree (−5.2854 eV) and −0.12799 (−3.4829 eV), respectively, and those of the β orbitals are −0.19292 (−5.2497 eV) and −0.12805 (−3.4845 eV), respectively, showing the energy differences are less than 0.04 eV. Therefore, we conclude that it is safe to compare only one of these orbitals to the nickel derivative, **4**, in the following discussion. Figure 3 demonstrates that the MOs of **3** and **4** are generally localized on either the TBTAC or C_{60} moieties. For example, the HOMOs and LUMO+3′s localize on the TBTAC and C_{60} skeleton, respectively. The TBTAC-centered HOMO and LUMO+4 of **3** are calculated to have lower energies compared to those of **4**. On the other hand, the C_{60}-centered MOs such as the LUMO+1 of **3** and LUMO of **4**, and the LUMO+3 show no significant energy shifts. These observations are consistent with the result that the VO formally functions as a moderate

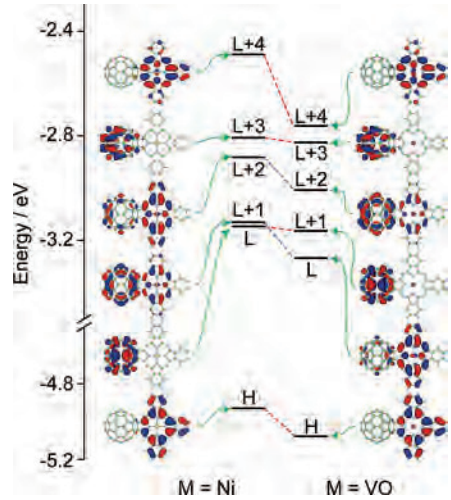

Figure 3. Selected frontier MOs of **4** (M = Ni, left) and **3** (M = VO, right) conjugates. Note the LUMO+1 of **4** is stabilized to the LUMO for **3**.

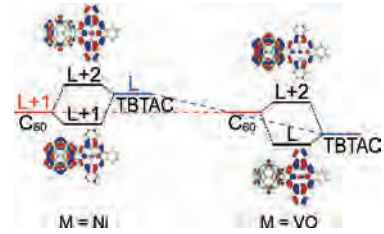

Figure 4. Schematic drawings showing how the TBTAC and C_{60} moieties interact for **3** (right) and **4** (left). Although only the α orbitals are shown here for **3**, the energy differences between the α and β orbitals are very small (see text).

electron-withdrawing unit. Since the TBTAC skeleton is directly affected by the VO while the C_{60} unit is not, the TBTAC-centered MOs are stabilized more than the C_{60}-centered MOs. In our previous paper, we described that the LUMO+1 and LUMO+2 of **4** delocalize over the entire molecule, and these can be expressed as the linear combinations of the corresponding MOs of the constituting units.[7] Similar to **4**, **3** also shows delocalized MOs for the LUMO and LUMO+2. However, in this case, the lower and higher energy levels (the LUMO and LUMO+2, respectively) are dominated by the TBTAC and C_{60} moieties, respectively.

Figure 4 illustrates how the delocalized MOs of the conjugates are generated by the linear combinations of MOs of the constituting units. In the case of **4**, the LUMO+1 of the C_{60} and the LUMO of the TBTAC have the same symmetry and are energetically close. Since the C_{60}-centered MO is lower in energy than the TBTAC-centered MO, the C_{60}-dominated LUMO+1 and TBTAC-dominated LUMO+2 are generated (Figure 4, left). By changing the central metal to VO, i.e. **3**, the TBTAC-centered MOs are stabilized. As a result, the lower delocalized MO is rather dominated by the TBTAC moiety, and the MO coefficients distributed on the TBTAC become small for the LUMO+2 (Figure 4, right). These two MOs are parallel to each other, since they are generated from different linear combinations of the same components. Therefore, the observed lowest energy band at 810 nm can be assigned mainly as the HOMO to LUMO transition. Although the second lowest Q-band detected at

(15) (a) Handa, M.; Suzuki, A.; Shoji, S.; Kasuga, K.; Sogabe, K. *Inorg. Chim. Acta* **1995**, *230*, 41. (b) Lever, A. B. P.; Licoccia, S.; Magnell, K.; Minor, P. C.; Ramaswamy, B. S. *Adv. Chem. Ser.* **1982**, *201*, 237.

(16) Note the redox couples of **5** shift positively by more than 500 mV with respect to **4**.

670 nm is obscured, this is assigned mainly as the HOMO to LUMO+2 transition. The negative MCD signals for these two bands also lend strong support to these assignments, and the positive MCD signals for the 650-nm band prove that this band is due to the HOMO to LUMO+4 transition perpendicular to the other two Q-components. Larger overlap integrals for the initial and final states of the 810-nm band compared to the 670-nm band are consistent with the experimental results. The HOMO to LUMO+1 or LUMO+3 transitions are essentially forbidden due to small overlap integrals between the initial and final states, indicating that the LUMO+1 and LUMO+3 are hardly involved in the Q-bands.

Conclusions

In the present study, we have synthesized the VO complex of a TBTAC−C_{60} conjugate, **3**, which shows large interunit MO interactions due to a close arrangement of the constituting units. The absorption spectrum of **3** is clearly different in shape from that of the nickel complex **4**, even though both compounds have identical peripheral substituents (OBu group) and aromatic skeleton. Although the absorption spectrum of **3** is apparently similar to that of the SO_2Bu-substituted nickel complex, **5**, the MCD spectra and band deconvolution analysis have revealed that the electronic structures are different. An electrochemical investigation demonstrated that VO withdraws electrons moderately more strongly than nickel. DFT calculations predict that the TBTAC-related MOs of **3** are substantially stabilized compared to **4**, while the C_{60}-centerd MOs are not significantly perturbed, being consistent with the electrochemical data. The spectroscopic features observed in this study suggest that the electronic structures of the TBTAC−C_{60} conjugates depend significantly on their central metals. Although many porphyrin−C_{60} and Pc−C_{60} conjugates have been reported to date, modification of the electronic mixing states of a conjugate by changing the central metal has not been shown previously.

Acknowledgment. This research was supported by a Grant-in-Aid for Young Scientists (B) No. 17750029 and that for Exploratory Research No. 19655045 from the Ministry of Education, Culture, Sports, Science, and Technology, Japan. T.F. is grateful to the Exploratory Research Program for Young Scientists from Tohoku University for their financial support. N.H. thanks the Sasakawa Scientific Research Grant from the Japan Science Society.

Supporting Information Available: Listings of FTIR (KBr) and ESI-FTICR mass spectrum of **3** (PDF). This material is available free of charge via the Internet at http://pubs.acs.org.

IC701840R